Vanadocalixarenes on Silica: Requirements for Permanent Anchoring and Electronic Communication

Namal de Silva,[†] Son-Jong Hwang,[‡] Kathleen A. Durkin,[§] and Alexander Katz*,[†]

Department of Chemical Engineering and College of Chemistry, University of California—Berkeley, Berkeley, California 94720, and Division of Chemistry and Chemical Engineering, California Institute of Technology, Pasadena, California 91125

Received December 16, 2008

Grafted V(V)—calixarene complexes that are 1,3-disubstituted at the lower rim have been synthesized using an extraordinarily mild procedure, using the V(III)—calixarene precursor *p*-Bu^t—calix[4]—$(OMe)_2(O)_2$V—Cl (**1c**), which is subsequently grafted onto silica and, afterward, oxidized to yield material **2c**. The calixarene acts as a sterically bulky chelating ligand and enforces isolated pseudo-octahedral vanadium centers on silica, as ascertained by ^{51}V NMR spectroscopy and analysis of the UV/vis spectrum of materials after calixarene removal via calcination. ^{13}C CP/MAS NMR spectroscopy of **2c** reveals lack of a downfield-shifted ipso carbon resonance, which is strongly indicative of a high d-orbital electron density for the V metal centers in **2c**, a result that is expected on the basis of a proposed simple geometric model that is consistent with single-crystal X-ray crystallographic data of early transition metal metallocalixarenes. This result motivates future programming of grafted metal centers with chemical information using lower-rim 1,3-disubstituted calixarene substituents via RO→metal interactions (R = lower-rim substituent). In addition, the critical necessity of covalent interactions between support and metal for maintaining isolated and redox stable vanadium-containing active sites is demonstrated by comparison with weakly physisorbed V(V)—calixarene complexes at similar surface densities. These rely on the noncovalent interactions of molecular precursor *p*-Bu^t—calix[4]—$(OMe)(O)_3$V═O (**1n**) with the surface of partially dehydroxylated silica yielding material **2n**. Unlike the redox and configurationally stable sites in material **2c**, vanadocalixarene species in **2n** aggregate and undergo reduction, as observed via EPR spectroscopy, ultimately leading to mixed V oxidation states as detected via near-infrared spectroscopy.

Introduction

Inspired by the catalytic proficiency and enantioselectivity of isolated VO_4 sites in vanadium bromoperoxidase enzymes[1] and synthetic approaches for enantioselective heterogeneous epoxidation catalysis,[2,3] it is of general interest to synthesize heterogeneous catalysts consisting of a permanent organic ligand coordination sphere around a vanadium cation, which persists even in the midst of ligand exchange processes, such as those that are known to be prevalent in catalysis mechanisms. There are relatively few examples of such materials[4] compared with the vast literature of conventional VO_4 sites immobilized on inorganic oxide supports.[5−9] These latter-type inorganic materials have been used extensively as catalysts for a variety of reactions, such as partial oxidation of methanol to formaldehyde,[5] selective catalytic reduction,[6] and oxidative dehydrogenation of hydrocarbons,[7] and have shown in certain cases a pronounced increase in catalytic turnover frequency when using isolated rather than aggregated vanadium sites.[8] The degree of vanadium site isolation when supported on silica and the oxygen ligand coordination geometry in such anchored sites have been thoroughly investigated using a variety of spectroscopic methods.[9]

[†] Department of Chemical Engineering, University of California.
[‡] California Institute of Technology.
[§] College of Chemistry, University of California.

(1) Anderson, M.; Willetts, A.; Allenmark, S. *J. Org. Chem.* **1997**, *62*, 8455–8458.
(2) Meunier, D.; Piechaczyk, A.; de Mallmann, A.; Basset, J. M. *Angew. Chem.* **1999**, *38, 23*, 3540–3542.
(3) Meunier, D.; de Mallmann, A.; Basset, J. M. *Top. Catal.* **2003**, *23, 14*, 183–189.
(4) (a) Rice, G. L.; Scott, S. L. *Langmuir* **1997**, *13*, 1545–1551. (b) Deguns, E. W.; Taha, Z.; Meitzner, G. D.; Scott, S. L. *J. Phys. Chem. B* **2005**, *109*, 5005–5011. (c) Grasser, S.; Haebner, C.; Kohler, K.; Lefebevre, F.; Basset, J.-M. *Phys. Chem. Chem. Phys.* **2003**, *5*, 1906–1911. (d) Tada, M.; Kojima, N.; Izumi, Y.; Tanaiike, T.; Iwasawa, Y. *J. Phys. Chem. B* **2005**, *109*, 9905–9916.
(5) (a) Deo, G.; Wachs, I. E. *J. Catal.* **1994**, *146*, 323–334. (b) Baltes, M.; Cassiers, K.; Van Der Voort, P.; Weckhuysen, B. M.; Schoonheydt, R. A.; Vansant, E. F. *J. Catal.* **2001**, *197*, 160–171. (c) Lim, S.; Haller, G. L. *Appl. Catal., A* **1999**, *188*, 277–286.
(6) Bond, G. C.; Tahir, S. F. *Appl. Catal.* **1991**, *71*, 1–31.
(7) (a) Tilley, T. D. *J. Mol. Catal. A: Chem.* **2002**, *182−183*, 17–24. (b) Gao, X.; Banares, M. A.; Wachs, I. E. *J. Catal.* **1999**, *188*, 325–331. (c) Wachs, I. E.; Jehng, J. M.; Deo, G.; Wechkuysen, B. M.; Guliants, V. V.; Benzinger, J. B.; Sundaresan, S. *J. Catal.* **1997**, *170*, 75–88.
(8) (a) Christodoulakis, A.; Machli, M.; Lemonidou, A. A.; Boghosian, S. *J. Catal.* **2004**, *222*, 293–306. (b) Karakoulia, S. A.; Triantafyllidis, K. S.; Tsilomelekis, G.; Boghosian, S.; Lemonidou, A. A. *Catal. Today* **2009**, *141*, 245–253.
(9) (a) Burcham, L. J.; Deo, G.; Gao, X.; Wachs, I. E. *Top. Catal.* **2000**, *11/12*, 85–100. (b) Olthof, B.; Khodakov, J.; Bell, A. T.; Iglesia, E. *J. Phys. Chem. B* **2000**, *104*, 1516–1528. (c) Wang, C.-B.; Deo, G.; Wachs, I. E. *J. Catal.* **1998**, *178*, 640–648. (d) Zhang, Q.; Yang, W.; Wang, X.; Wang, Y.; Shishido, T.; Takehira, K. *Microporous Mesporous Mater.* **2005**, *77*, 223–234. (e) Zhang, S. G.; Higashimoto, S.; Yamashita, H.; Anpo, M. *J. Phys. Chem. B* **1998**, *102*, 5590–5594. (f) Lacheen, H. S.; Iglesia, E. *J. Phys. Chem. B* **2006**, *110*, 5462–5472. (g) Gao, X.; Bare, S. R.; Weckhuysen, B. M.; Wachs, I. E. *J. Phys. Chem. B* **1998**, *102*, 10842–10852.

10.1021/cm803392m CCC: $40.75
Published on Web 04/14/2009

Surface complexes rely on grafting strategies for covalently anchoring vanadium to a support material such as silica. Scott and co-workers[4a,b] demonstrated the synthesis of well-defined $\equiv SiOVOX_2$ surface complexes, which are synthesized via reaction of homogeneous $O{=}VX_3$ ($X = Cl$, O^iR) precursors with a silanol-containing silica surface, causing formation of a covalent Si−O−V bond on the surface and concomitant liberation of HCl. Basset et al.[4c] synthesized V(IV) complexes grafted onto the surfaces of silica, alumina, and titania using the amido precursor $V[N(CH_3)_2]_4$. These latter two examples nicely demonstrate approaches for covalently anchoring V(V) and V(IV) species to the inorganic oxide surface. The ensuing surface complexes are hydrolytically unstable and lead to oligomerization upon exposure to traces of moisture. Tilley et al.[10] have developed robust tethering strategies for synthesis of organic−inorganic hybrid materials consisting of decavanadate anions exchanged onto covalently tethered propylammonium cations on silica. These materials have been used as intermediates, which, after calcination, yield highly dispersed V sites on silica.[10] Other hybrid organic−inorganic heterogeneous vanadium catalysts have used bulky ligands to control enantioselectivity. For example, the system reported by Tada and co-workers[4d] consists of immobilized V(IV) Schiff base metal complexes on the surface of silica. These complexes are reported to self-dimerize on the surface via hydrogen bonding between phenol and carboxylate functional groups on the ligand based on X-ray absorption spectroscopy[4d] and exhibit a highly broadened EPR spectrum that is consistent with nonisolated vanadium sites.[11]

The goal of this study is to develop a generalizable approach for the synthesis of hydrolytically stable and site-isolated anchored V(V) sites, which consist of a permanent organic ligand coordination sphere surrounding the metal cation. This approach is motivated by our previously reported synthesis of anchored Ti(IV)−calixarene surface complexes on silica,[12] which have been demonstrated to be single-site heterogeneous catalysts in which the calixarene enforces a specific coordination environment around the metal center and has a profound effect on metal cation's Lewis acidity.[12a] Our strategy uses a bulky calixarene ligand to isolate V(V) centers on the surface and define a fixed coordination geometry surrounding them.

We wish to address whether there is a critical requirement for covalent V−O−Si connectivity in order to maintain vanadium site isolation of anchored active sites in immobilized vanadocalixarene materials. Our hypothesis is that such a covalent bond may be required to prevent oligomerization of anchored vanadium active sites, even when using sterically bulky ligands such as calixarenes and low active site surface densities.

Two contrasting immobilization approaches based on this concept are investigated in order to ultimately understand the importance of grafting versus noncovalent physisorption as driving forces for anchoring and achieving isolated V(V)-containing active sites. Both of these approaches rely on previously reported vanadocalixarene precursors, *p*-Bu^t−calix[4]−$(OMe)_2(O)_2V$−Cl (**1c**)[13a] and *p*-Bu^t−calix[4]−$(OMe)(O)_3V{=}O$ (**1n**),[13b] which have been characterized using single-crystal X-ray diffraction. The selection of these two precursors is based upon the contrasting structural features relevant to their anchoring capabilities. Precursor **1c** contains a chloro linker that can undergo direct reaction with silanol groups, as demonstrated previously for vanadium surface complexes,[4a,b] whereas **1n** lacks a clearly defined leaving group for grafting. The covalent approach is represented in Scheme 1 and uses *p*-Bu^t−calix[4]−$(OMe)_2(O)_2V$−Cl (**1c**) as a precursor for materials synthesis, leading to covalent material **2c**, whereas the physisorption approach is represented in Scheme 2 and uses *p*-Bu^t−calix[4]−$(OMe)(O)_3V{=}O$ (**1n**), leading to material **2n**. Critically, in this paper, we also investigate the repercussions of having a disubstituted versus monoosubstituted lower rim in the calixarene as ligand, in terms of enhancing electronic communication between calixarene lower-rim substituents and the metal center. We develop an analysis based on simple geometric arguments that span different early transition metals and ligands to demonstrate that such an enhancement is expected for lower-rim disubstituted calixarene ligands on the basis of distances between methoxy oxygens and metal. Finally, though the lower-rim substituents used here are achiral methoxy groups, chiral substituents, in which the asymmetric center is directly connected to calixarene lower-rim oxygens, are currently being explored by exploiting the synthetic tailorability of calixarenes as molecular scaffolds.[14] This relies on the use of C_2 symmetric calixarenes as ligands, as described in this paper, since ligands with this symmetry are desirable from the standpoint of chiral catalyst active sites.[15]

Results and Discussion

Mild conditions relying on V(III) complexes are used to synthesize materials consisting of covalently anchored vanadocalixarene sites on silica. The weakly Lewis acidic nature of V(III) during materials synthesis under oxygen-free conditions facilitates the use of a variety of substituents on the calixarene lower rim, which are otherwise expected to be unstable to decomposition, as observed in the presence of stronger Lewis acids via intramolecular ether cleavage, in the presence of Ti(IV)[16] or V(V) cations (see experimental conditions for synthesis of **1n** utilizing this cleavage reaction). The synthesis involves stirring a green toluene solution of precursor **1c** in the presence of pretreated silica. The resulting green solid is washed thoroughly with toluene and dried under vacuum. The

(10) Hess, C.; Hoefelmeyer, J. D.; Tilley, T. D. *J. Phys. Chem. B* **2004**, *108*, 9703–9709.
(11) Chiesa, M.; Meynen, V.; Van Doorslaer, S.; Cool, P.; Vansant, E. F. *J. Am. Chem. Soc.* **2006**, *128*, 8955–8963, and references therein.
(12) (a) Notestein, J. M.; Iglesia, E.; Katz, A. *J. Am. Chem. Soc.* **2004**, *126*, 16478–16486. (b) Notestein, J. M.; Iglesia, E.; Katz, A. *Chem. Mater.* **2007**, *19*, 4998–5005.
(13) (a) Castellano, B.; Solari, E.; Floriani, C.; Re, N.; Chiesi-Villa, A.; Rizzoli, C. *Organometallics* **1998**, *17*, 2328–2336. (b) Castellano, B.; Solari, E.; Floriani, C.; Scopelliti, R.; Re, N. *Inorg. Chem.* **1999**, *38*, 3406–3413.
(14) Solovyov, A.; Notestein, J. M.; Durkin, K. A.; Katz, A. *New J. Chem.* **2008**, *32*, 1314–1325.
(15) Yoon, T. P.; Jacobsen, E. N. *Science* **2003**, *299*, 1691–1693.
(16) Zanotti-Gerosa, A.; Solari, E.; Giannini, L.; Floriani, C.; Re, N.; Chiesi-Villa, A.; Rizzoli, C. *Inorg. Chim. Acta* **1998**, *270*, 298–311.

Scheme 1. Reaction Sequence for Grafting[a]

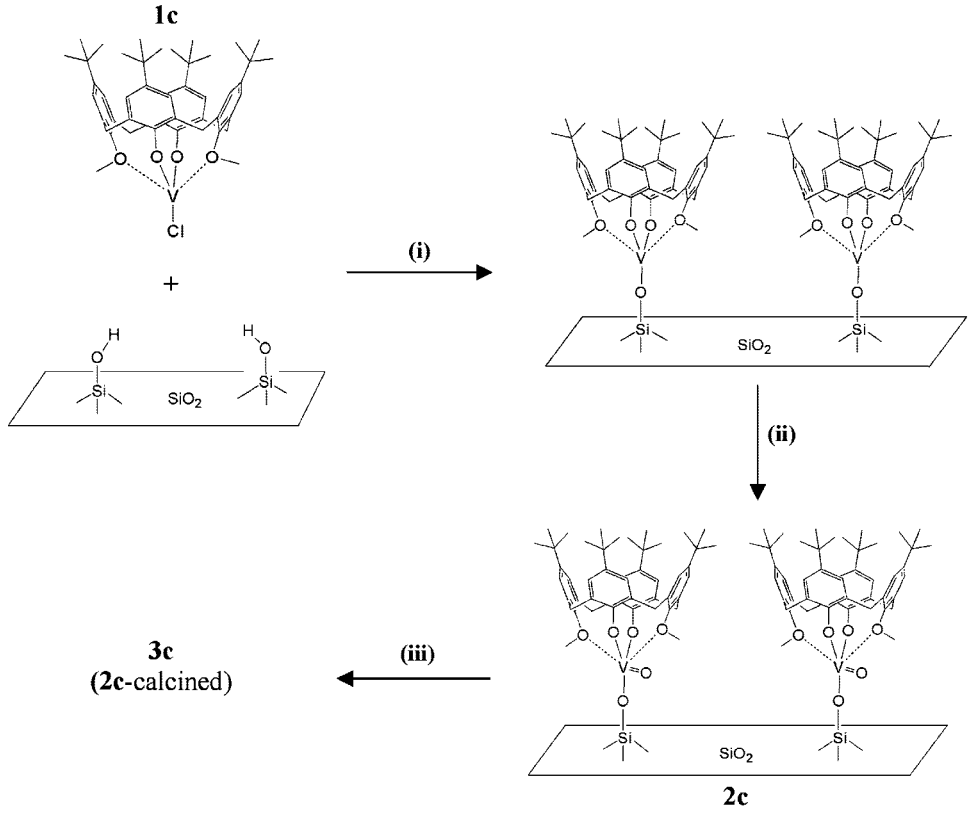

[a] (i) Stir in toluene, filter, wash, and dry under vacuum (all steps under air-free conditions). (ii) Exposure to ambient air. (iii) Heat up to 550° C in dry synthetic air/O_2 at a ramp rate of 5 °C/min.

Scheme 2. Reaction Sequence for Noncovalent Immobilization[a]

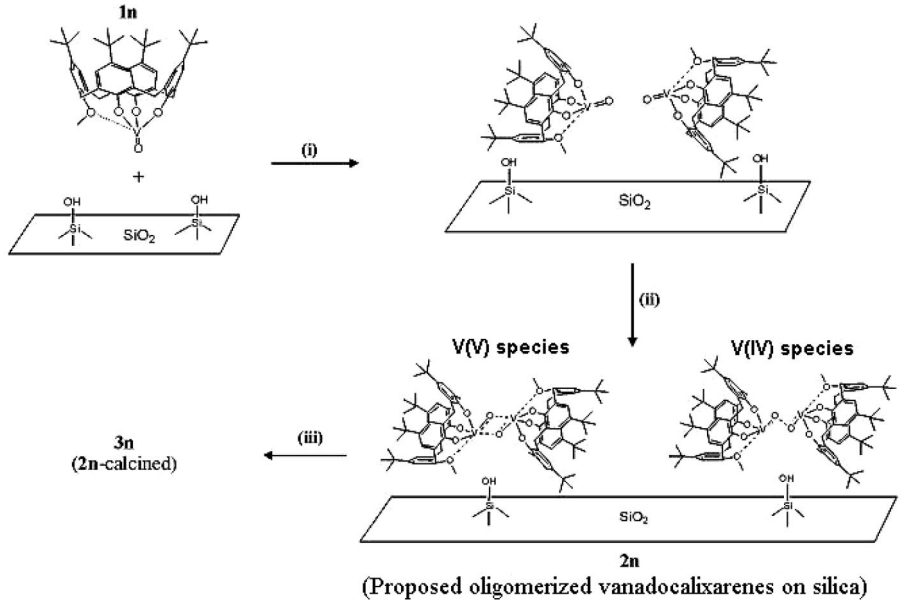

[a] (i) Stir in hexane, filter, wash with hexane, and dry under vacuum (all steps under air-free conditions). (ii) Exposure to ambient air. (iii) Heat up to 550° C in dry synthetic air/O_2 at a ramp rate of 5 °C/min.

covalent connectivity between the immobilized vanadocalixarene complex and silica in **2c** is demonstrated by the lack of observed leaching upon exhaustive washing of **2c** with an excess of toluene, since in the absence of this connectivity, as in **3n**, calixarene leaching occurs under these conditions (vide infra). This observation is consistent with the grafting of **1c** via reaction of chloro and silanol groups with concomitant release of HCl, as observed in other closely related surface complexes of early transition metals.[4a,b,12a,19,20a] We have previously demonstrated the irreversibility of such an anchoring strategy via the difficulty of cleaving grafted metallo-

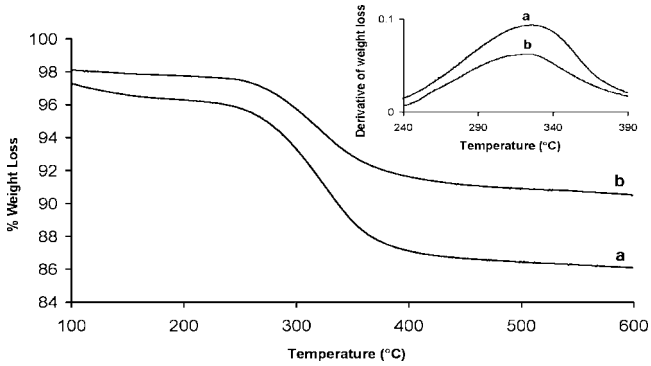

Figure 1. Thermogravimetric analysis of (a) **2c** and (b) **2n**.

Table 1. Summary of Materials Synthesized[a]

material	μmol V g^{-1}	V (wt %)	V nm^{-2}	calixarene:V
2c	129	0.66	0.15	1.04
2n	88	0.45	0.11	1.19[b]

[a] Determined by ICP-MS. [b] Reported as an upper-bound due to the presence of residual solvent in the noncovalent material.

calixarenes from the silica surface, requiring high concentrations and large excesses of HCl.[20a]

Upon exposure to ambient air, the color of the material gradually changes from green to brown, representative of vanadium center oxidation and synthesis of material **2c**, as shown in Scheme 1. It is known that both homogeneous and heterogeneous V(III) metal complexes are spontaneously oxidized to the corresponding V(V) complexes in the presence of molecular oxygen.[17] In a recent theoretical study, Goodrow and Bell proposed a mechanism regarding the oxidation of intermediate V(III) centers on silica, in which reoxidation proceeds via adsorption of O_2 to form a surface-bound peroxo species that migrates via support oxygens to eventually oxidize another V(III) center.[18] This oxygen transport via surface enables a four-electron oxidation of two anchored V(III) sites while avoiding the necessity of V−O−V connectivity that is expected to be absent in **2c**. The kinetics of this oxidation process is beyond the scope of the current investigation.

The amount of calixarene combusted via thermogravimetric analysis of **2c** is shown in Figure 1a and agrees well with elemental analysis data, yielding a calixarene to vanadium ratio of near unity when analyzed in conjunction with V ICP/MS analysis. This ratio is represented in Table 1 and strongly suggests covalent connectivity between vanadium and calixarene in **2c**. Further evidence for such connectivity is present in the diffuse reflectance UV−vis spectrum of hydrated **2c**, which is shown in Figure 2 and is dominated by strong calixarene→V(V) ligand-to-metal charge-transfer (LMCT) bands in the range between 2.0 and 2.8 eV. These bands are also observed for other d^0 metallocalixarene complexes such as **1n** and are similar in energy to previously reported LMCT bands of grafted Ti(IV)−calixarene materials.[12] The LMCT

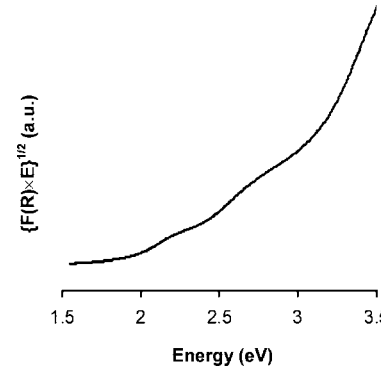

Figure 2. Diffuse reflectance UV−visible absorption spectra of **2c**.

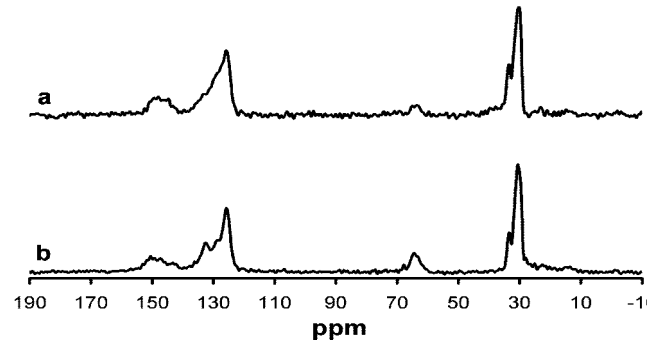

Figure 3. ^{13}C CP/MAS NMR of (a) **2n** and (b) **2c**.

bands of **2c** shown in Figure 2 remain unchanged upon aging in the presence of atmospheric moisture, suggesting a stable vanadium−calixarene coordination environment. These bands disappear completely upon calcination for **3c**, however, further substantiating their nature as LMCT bands, and the only band remaining for **3c** corresponds to oxygen to vanadium charge transfer for isolated VO_4 sites on silica.

A new synthetic approach for **1n** was discovered, which enables its isolation in high purity and yield and its use as a precursor for **2n** synthesis as required in Scheme 2, and facilitates characterization of **1n** via ^{13}C NMR spectroscopy, as reported below. During noncovalent immobilization of **1n** onto silica, a dark brown hexane solution of **1n** is treated with partially dehydroxylated silica at room temperature under strictly anhydrous conditions. Spontaneous partitioning of **1n** to the silica surface is evident by the immediate transfer of the dark brown color of **1n** from solution to silica. The amount of calixarene combusted via thermogravimetric analysis of **2n** (Figure 1b) agrees closely with elemental analysis data, which when coupled with vanadium ICP/MS analysis yields a calixarene to vanadium ratio of approximately unity (Table 1). This suggests that the integrity of vanadium−calixarene connectivity is maintained in **2n**. However, in contrast to the covalent attachment of vanadocalixarenes in **2c** (vide infra), the noncovalent nature of calixarene attachment in **2n** is evident by the fact that a majority of anchored calixarene sites can be washed off from the solid surface using toluene, mainly in the form of the original precursor **1n**.

^{13}C CP/MAS NMR spectra are shown in Figure 3 for both materials **2c** and **2n** and provide structural information regarding the integrity of methoxy groups in **2c**. The ∼2:1 ratio of methoxy resonance areas (64 ppm) in the ^{13}C CP/

(17) (a) Groysman, S.; Goldberg, I.; Goldschmidt, Z.; Kol, M. *Inorg. Chem.* **2005**, *44*, 5073–5080. (b) Horvath, B.; Strutz, J.; Geyer-Lippmann, J.; Horvath, E. G. *Z. Anorg. Allg. Chem.* **1981**, *483*, 181–192. (c) Venkov, T. V.; Hess, C.; Jentoft, F. C. *Langmuir* **2007**, *23*, 1768–1777.
(18) Goodrow, A.; Bell, A. T. *J. Phys. Chem. C* **2007**, *40*, 14753–14761.
(19) Notestein, J. M.; Solovyov, A.; Andrini, L. R.; Requejo, F. G.; Katz, A.; Iglesia, E. *J. Am. Chem. Soc.* **2007**, *129*, 15585–15595.

Scheme 3. Geometrical requirements for stronger MeO→M interactions[a]

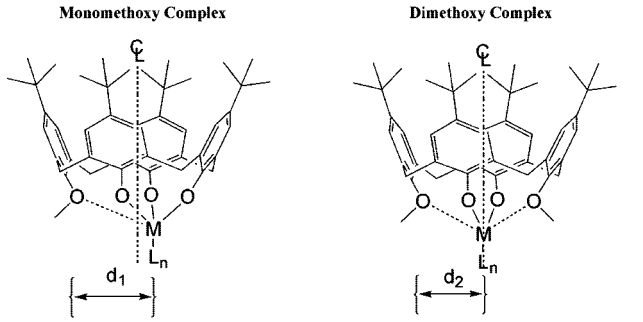

[a] Geometry requires $d_2 < d_1$; stronger MeO→M interactions are predicted for dimethoxy- versus monomethoxycalixarene complexes.

MAS NMR spectrum of **2c** relative to **2n** indicates that both methoxy substituents in **2c** survive materials synthesis and the mild Lewis acidity of the V(III) center that is used in the anchoring scheme. The resulting vanadocalixarenes in **2c** are the first grafted calixarenes to contain two methoxy donors to the metal center, in comparison with the single methoxy **2n** and previously synthesized titanocalixarenes on inorganic oxide supports.[12] The presence of two methoxy donor groups in **2c** enforces a C_2 ligand geometry that is desirable for enantioselective catalyst synthesis[15] (vide supra) and is expected to substantially increase the d-orbital electron density on the vanadium metal center.

A higher d-orbital electron density for vanadium centers in **2c** relative to **1n** is predicted on the basis of simple geometric arguments outlined in Scheme 3. This is because increased electron donation to the metal center via MeO→metal interactions between substituted calixarene lower-rim oxygens and metal are more prevalent when using a 1,3-dimethoxy relative to a monomethoxy calixarene ligand. This is due to two factors. First, the shear number of MeO→metal interactions has increased in the dimethoxy system 2-fold, resulting in placing the metal within a pseudo-octahedral coordination environment. Second, geometrical constraints enforced by the rigid macrocyclic nature of the calixarene require that d_2 be less than d_1 in Scheme 3, so that the strength of each MeO→metal interaction contributing in the case of the dimethoxy system is significantly larger relative to the monomethoxy case. To verify this latter distance prediction, Figure 4 is a compilation of MeO−metal bond distances, as measured via single-crystal X-ray diffraction, for all Ti and V complexes that consist of relatively undistorted covalent calix−O−metal bonds, measured to be 1.80−1.83 Å for Ti and 1.74−1.82 Å for V. Density functional theory calculations are included in Figure 4 in order to estimate MeO−metal bond distances for complexes that have not been structurally characterized, as well as to corroborate experimental measurements. These calculations of MeO−metal distances are observed to characteristically overestimate experimentally measured MeO−metal distances by ∼0.1 Å. The results in Figure 4 demonstrate a clear trend: 1,3-dimethoxycalixarene complexes have on average a ∼0.2 Å shorter MeO−metal distance relative to monomethoxycalixarene complexes, independent of metal and ligand type and metal oxidation state.

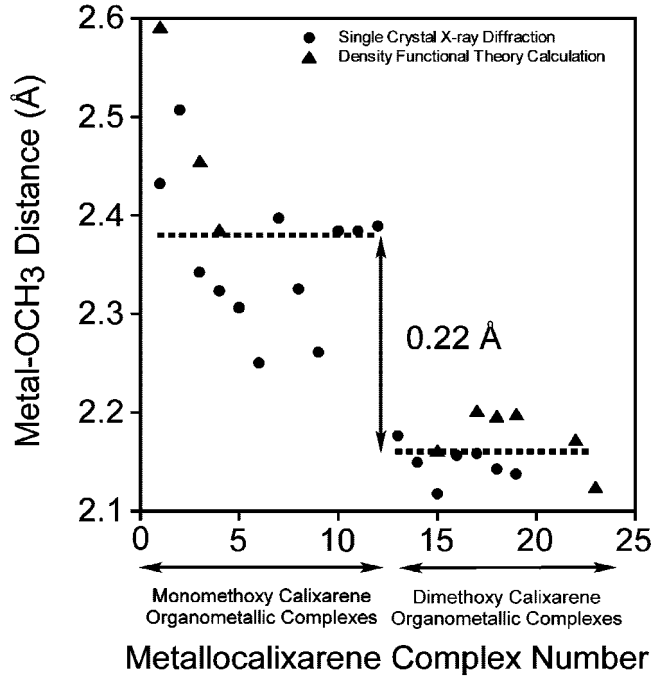

Figure 4. Compilation of MeO−metal bond distances as measured by single-crystal X-ray diffraction and calculated by density functional theory (see Supporting Information, Table S1, for the corresponding structures).

This general conclusion is also borne out when analyzing the most directly relevant complexes to those of this paper, **1n** and **1c**, as well as Ti analogs **1′** and **2′**, in Table 2. Comparison of structures **1n** and **1c** demonstrates a 0.19 Å shorter MeO−V dative bond distance for the dimethoxy system. This result is contrary to the predicted trend on the basis of metal formal charge. Dimethoxycalixarene complex **3′** in Table 2 has the same formal charge as **1n** on vanadium, and though not reported experimentally, an upper bound for the MeO−V distance in **3′** was estimated using density functional theory. This estimate demonstrates that the MeO−V distance in **3′** is at least 0.22 Å shorter than that for the monomethoxy complex **1n**. A similar comparison for **1′** and **2′** yields a 0.30 Å shorter MeO−Ti dative bond distance for the dimethoxy system. On the basis of the evidence above, the vanadium center in **2c** is also predicted to have strong contributions to d-orbital electron density due to MeO→metal interactions, relative to complex **1n**, and the two methoxy donors in **2c** are predicted to make for interesting comparisons catalytically with previously reported grafted Ti(IV)−calixarenes on inorganic oxide supports,[12,19,20] which are all based on monomethoxy calixarene ligands.

NMR spectroscopy can be used to provide indirect evidence for increased d-orbital electron density in **2c**. The entire lack of a downfield shift in the ipso carbon resonance

(20) (a) Notestein, J. M.; Andrini, L. R.; Kalchenko, V. I.; Requejo, F. G.; Katz, A.; Iglesia, E. *J. Am. Chem. Soc.* **2007**, *129*, 1122–1131. (b) Katz, A.; Da Costa, P.; Lam, A. C. P.; Notestein, J. M. *Chem. Mater.* **2002**, *14*, 3364–3368.

Table 2. Selected MeO−Metal Distances for Metallocalixarene Complexes for V and Ti

Complex	Structure	MeO-metal Distance (Å)	Ref.
1n	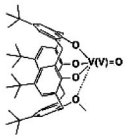	2.34	13b
1c	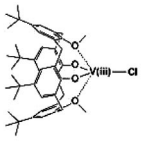	2.15	13a
3'	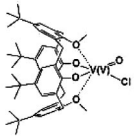	2.12 (Upper Bound)	DFT (This work)
1'	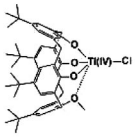	2.42	16
2'	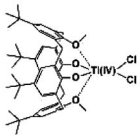	2.12	28

(i.e., above 155 ppm) is observed for grafted Si(IV)−*tert*-butylcalixarene sites on silica, as these sites do not have accessible d-orbitals and also lack calixarene to metal LMCT bands in these materials.[20b,12a] This downfield shift is observed, however, for the analogous grafted Ti(IV)−*tert*-butylcalixarenes on silica, which contain unoccupied d orbitals manifested in the LMCT band of these materials and strong Lewis acidity in catalysis.[12a]

Examination of the ^{13}C CP/MAS NMR spectrum of material **2c** in Figure 3b shows a critical lack of an ipso carbon resonance above 155 ppm, characteristic of what would be expected for an octahedral V(V) metal center with high d-orbital electron density. This is in stark contrast to results with the V(V) monomethoxycalixarene complex **1n**, in which the ipso carbon resonances observed in the ^{13}C NMR spectrum are shifted downfield at 160−162 ppm in deuterated chloroform. The data above provide critical evidence for high d-orbital electron density of the vanadium metal center in **2c**.

Evidence for isolated vanadium centers in **2c** is observed in the diffuse-reflectance UV−vis spectrum of hydrated **3c**, as shown in Figure 5a, which exhibits an edge energy of 3.1 eV. This value of the edge energy is higher than that previously reported for hydrated, highly dispersed vanadium on silica materials, which have been reported to be ∼2.2 eV for low-coverage materials consisting of 0.5 V/nm^2 and is slightly lower than the value of ∼3.8 eV reported for dehydrated isolated vanadium on silica xerogel materials.[21] The comparatively large value of the edge energy[9g,22] in hydrated **3c** suggests isolated vanadium sites in uncalcined precursor material **2c** and further suggests that the bulky and

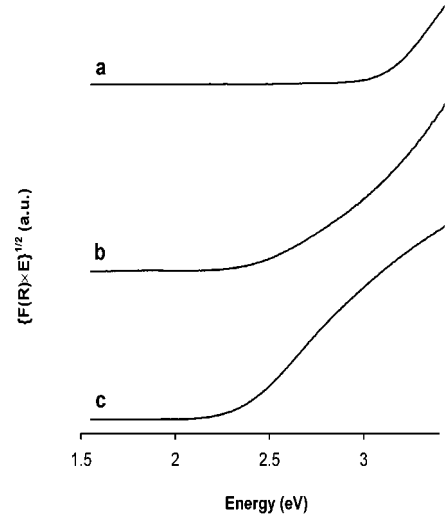

Figure 5. Diffuse reflectance UV−visible absorption edge energy spectra for (a) **3c**, calcined, as-made **2c** (spectra of calcined, aged **2c** and calcined, as-made **2c** are identical); (b) **3n**, calcined, as-made **2n**; and (c) **3n**, calcined, aged **2n**.

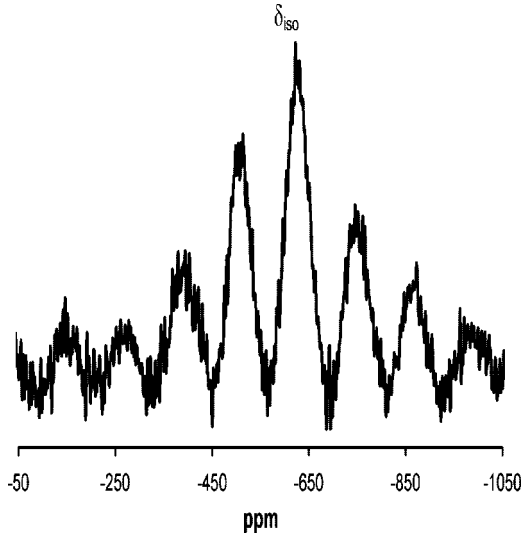

Figure 6. ^{51}V MAS NMR spectrum of **3c**.

tripodal calixarene ligand in **2c** facilitates site isolation of covalently anchored vanadium sites.

Additional evidence for site isolation in covalent materials is observed in the ^{51}V MAS NMR spectrum of hydrated **3c**, which is shown in Figure 6. The value of δ_{iso} of −627 ppm for hydrated **3c** is consistent with the range of δ_{iso} values from −520 to −710 ppm reported for hydrated anchored V(V) within a distorted tetrahedral environment on silica.[23] Similar δ_{iso} ranges have been observed in model compounds such as $(Ph_3SiO)_3V{=}O$,[23c] whereas distorted octahedral V species in V_2O_5[23d] are associated with δ_{iso} values in the range −200 to −400 ppm. The ^{51}V NMR spectrum of dehydrated **3c** at T = 130 °C exhibits a similar ^{51}V NMR spectrum and

(21) (a) Rulkens, R.; Male, J. L.; Terry, K. W.; Olthof, B.; Khodakov, A.; Bell, A. T.; Iglesia, E.; Tilley, T. D. *Chem. Mater.* **1999**, *11*, 2966–2973. (b) Tran, K.; Stiegman, A. E.; Scott, G. W. *Inorg. Chim. Acta* **1996**, *243*, 185–191. (c) Tran, K.; Hanning-Lee, M. A.; Biswas, A.; Stiegman, A. E.; Scott, G. W. *J. Am. Chem. Soc.* **1995**, *117*, 2618–2626.

(22) Gao, X. J.; Wachs, I. E. *J. Phys. Chem. B* **2000**, *104*, 1261–1268.

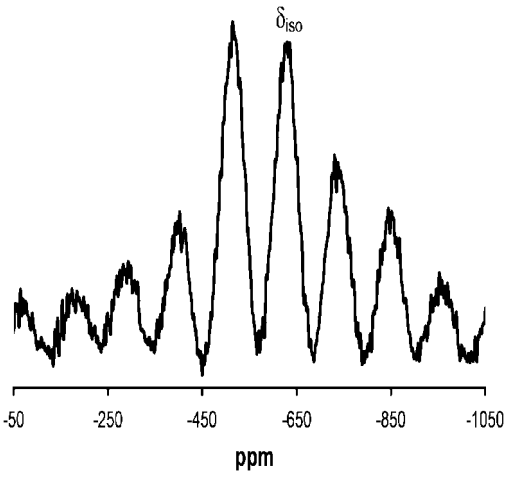

Figure 7. ^{51}V MAS NMR spectrum of **2c**.

δ_{iso} of −629 ppm. This is in contrast to observed increases in the octahedral vanadium region when comparing hydrated and dehydrated anchored vanadium centers on silica, which have been observed even for materials consisting of 0.5 mol % V (smaller loadings than in **2c**).[23a] This observation suggests that the particular metal precursor and synthetic route used significantly affect the hydrolytic stability of anchored V(V) active sites on silica in calcined materials.

The ^{51}V NMR spectrum of isolated vanadocalixarene active sites comprising hydrated **2c** have a δ_{iso} of −630 ppm in Figure 7. The value of this chemical shift is similar to that of a previously reported grafted vanadium alkoxide complex on silica,[4a] which consists of V(V) within an oxo environment and monopodally attached to the silica surface, as in **2c**. However, this similarity is likely accidental, as the ^{51}V NMR chemical shift in **2c** is expected to be influenced by, among other effects, (i) three calixarene phenoxy ligands being different from alkoxy and siloxy ligands (the latter two ligands were shown to have a similar effect on the ^{51}V NMR chemical shift of V(V) complexes)[4a] as well as (ii) the two MeO→V bonds in **2c**. The convoluted effect of contributions i and ii above can be partially ascertained by comparing the chemical shift of **1n** of −358 ppm to that of V(═O)(^{i}OPr)$_3$ reported previously[4a] at −630 ppm.

On the basis of group contribution reasoning, replacement of one of the calixarene phenoxy ligands of **1n** with a siloxy ligand in **2c** would be expected to have the effect of decreasing the ^{51}V chemical shift of **2c** relative to **1n** via the similar effects of alkoxy and siloxy ligands in this regard (vide supra). The combination of this effect and the effect ii may cause the ^{51}V resonance chemical shift of **2c** to decrease from its value in **1n** to the point of overlap with that of other vanadium complexes on silica[4a,23] and V(═O)(^{i}OPr)$_3$.[4a]

In contrast to behavior observed with **3c**, dehydration of **2c** leads to an almost complete disappearance of ^{51}V NMR signal intensity in Figure 8b, which reappears upon hydration, as shown in Figure 8c. This appearance/disappearance of the ^{51}V NMR spectrum upon hydration/dehydration signifies a highly anisotropic environment surrounding the V nucleus upon dehydration. Similar types of broadening in the ^{51}V MAS NMR spectrum upon dehydration have been observed in $(1 - x)K_2S_2O_7 \cdot xV_2O_5$ melts where $x = 0.1-0.3$. This phenomenon was correlated to a decreased mobility of VO_5 units in this class of materials as x increases.[23e] The observations in the ^{51}V MAS NMR spectrum of hydrated and dehydrated **2c** are consistent with a highly rigid and unique, asymmetric environment afforded by the anchored calixarene ligand around each vanadium metal center.

The required calixarene rigidity to bring about the observed broadening is consistent with the previously observed breadth of methylene resonances in the ^{13}C CP/MAS NMR spectrum of grafted calixarenes.[24] The covalent connectivity between V and calixarene during aging of **2c** in the presence of atmospheric moisture is maintained. Exhaustive washing with toluene of **2c** that had been aged for 4 months leads to a neglibile loss of calixarene (less than 10%), and the edge energy for such a calcined, aged **2c** is similar to the result obtained from calcining a freshly synthesized **2c** sample, shown in Figure 5. This requires a permanent covalent calixarene attachment in **2c** that is not affected by atmospheric moisture. In comparison with covalently grafted vanadocalixarene sites on silica in **2c**, calcination of **2n** leads to **3n**, which has a measurably lower edge energy of 2.8 eV when compared with **3c**. Aging of material **2n** in the presence of atmospheric moisture upon storage at room temperature during the course of 4 months leads to a material with an even lower edge energy of 2.4 eV after calcination. This suggests that vanadium centers in **2n** slowly interconvert to higher degrees of coordination consistent with VO_5 and VO_6 centers, whereas, in contrast, those in **2c** remain isolated in a pseudo-octahedral configuration, even in the presence of atmospheric moisture (vide supra).

Unlike stable material **2c**, the color of **2n** gradually converts from brown to green upon prolonged exposure to air. The ^{51}V MAS NMR spectrum of **2n** shows very weak intensity, which could be due either to quadrupolar interactions between aggregated V(V) centers or the presence of reduced species, which is in contrast to the intense resonances observed for **2c**.

The presence of a significant amount of reduced V(IV) species in **2n** is demonstrated via EPR spectroscopy, which has a 6-fold higher integrated EPR intensity when normalized per V site relative to material **2c**. The EPR spectrum shown in Figure 9 for **2n** is consistent with V(IV) centers and consists of characteristic isotropic signals[25] attributed to localized V(IV) species. The axial features in this spectrum consist of eight hyperfine lines, which result from the coupling of the d^1 electron to a single ^{51}V nucleus ($I = 7/2$).

(23) (a) Stiegman, A. E.; Eckert, H.; Plett, G.; Kim, S. S.; Anderson, M.; Yavrouian, A. *Chem. Mater.* **1993**, *5*, 1591–1594. (b) Morey, M.; Davidson, A.; Eckert, H.; Stucky, G. *Chem. Mater.* **1996**, *8*, 486–492. (c) Das, N.; Eckert, H.; Hu, H.; Wachs, I. E.; Walzer, J. F.; Feher, F. J. *J. Phys. Chem.* **1993**, *97*, 8240–8243. (d) Eckert, H.; Wachs, I. E. *J. Phys. Chem.* **1989**, *93*, 6796–6805. (e) Lapina, O. B.; Shubin, A. A.; Khabibulin, D. F.; Terskikh, V. V.; Bodart, P. R.; Amoureux, J.-P. *Catal. Today* **2003**, *78*, 91–104. (f) Fontenot, C. J.; Wiench, J. W.; Pruski, M.; Schrader, G. L. *J. Phys. Chem. B* **2001**, *105*, 10496–10504. (g) Fontenot, C. J.; Wiench, J. W.; Schrader, G. L.; Pruski, M. *J. Am. Chem. Soc.* **2002**, *124*, 8435–8444.

(24) Notestein, J. M.; Katz, A.; Iglesia, E. *Langmuir* **2006**, *22*, 4004–4014.

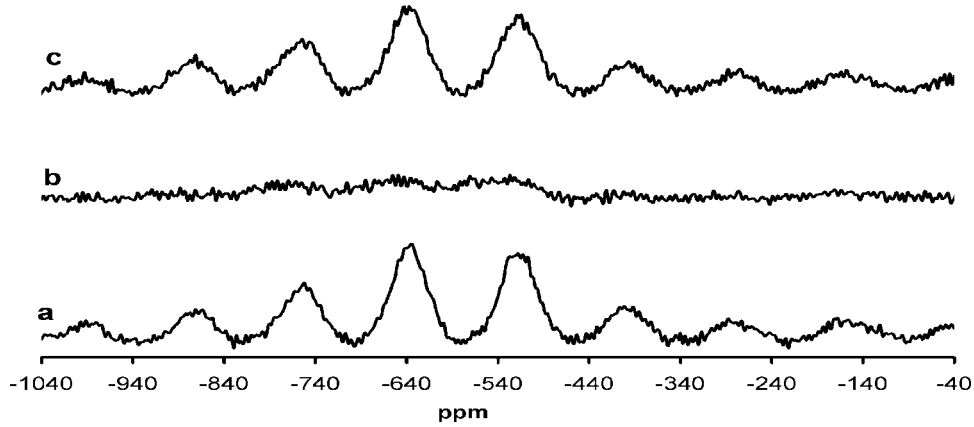

Figure 8. ^{51}V MAS NMR spectra of **2c**: (a) hydrated, (b) dehydrated, (c) rehydrated.

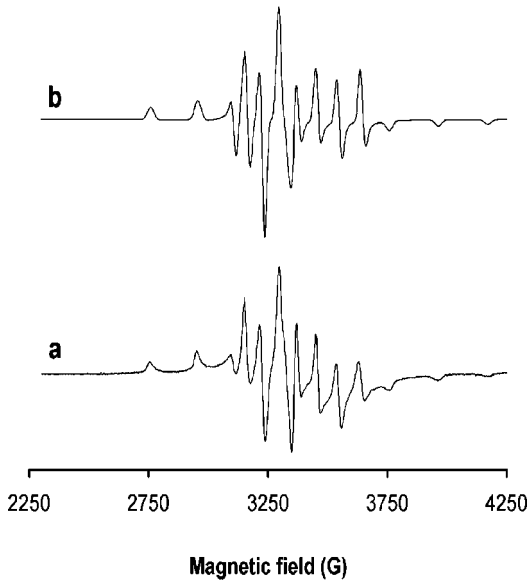

Figure 9. EPR spectra of **2n**: (a) experimental and (b) simulated.

Well-resolved hyperfine structures are indicative of a lack of communication between V(IV) centers, as extended clustering of vanadium species is usually implicated by a broad line that suppresses the hyperfine envelopes in the EPR spectrum.[25a] The simulated spectrum obtained for **2n** has the following tensor values: $g_{\|} = 1.933$, $g_{\perp} = 1.978$, $A_{\|} = 202$, and $A_{\perp} = 76$. These values for the *g*-tensor and hyperfine tensor are in close agreement with those of the oxovanadium (IV) ions within five or six coordinate environments having axial symmetry. Material **2n** also consists of mixed valence complexes, as indicated by an intervalence transition band in the near-infrared region,[26] at 830 nm, as shown in Figure 10. This transition is not observed in material **2c**. We propose that, in the absence of a covalent linkage, weakly physisorbed **1n** molecules in *noncovalently* grafted material **2n** transform into surface dimerized species,[27] which undergo subsequent reduction and oligomerization. Reduced species in **2n** may be generated via autoreduction to form a dimeric V(IV) peroxo-bridged species, one possibility of which is represented in Scheme 2. Related peroxo-bridged intermediates have been invoked to explain redox instablility of vanadocalixarene complexes in the presence of molecular oxygen involving a V(IV)−V(V) couple.[27] Due to the coordinative saturation postulated for immobilized **2n** within the dimeric intermediates of Scheme 2, a high d-orbital electron density for V centers in **2n** is predicted relative to **1n**. This is manifested by a lack of downfield-shifted ipso carbon resonances in the ^{13}C CP/MAS NMR spectrum of **2n** in Figure 3a.

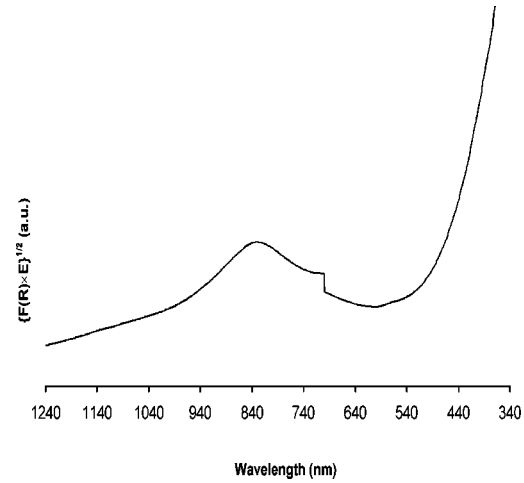

Figure 10. Diffuse reflectance UV−visible absorption edge energy spectra for aged **2n**.

Conclusions

Grafted vanadocalixarene complexes on silica have been synthesized via the covalent immobilization of vanadocalixarene *p*-Bu^t−calix[4]−$(OMe)_2(O)_2$V(III)−Cl (**1c**). This has

(25) (a) Baltes, M.; Van Der Voort, P.; Weckhuysen, B. M.; Rao, R. R.; Catana, G.; Schoonheydt, R. A.; Vansant, E. F. *Phys. Chem. Chem. Phys.* **2000**, *2*, 2673. (b) Ballhausen, C. J.; Gray, H. B. *Inorg. Chem.* **1962**, *1*, 111. (c) Kievelson, D.; Lee, S.-K. *J. Chem. Phys.* **1964**, *41*, 1896–1903. (d) Luan, Z.; Kevan, L. *J. Phys. Chem. B* **1997**, *101*, 2020–2017.

(26) (a) Tsuchida, E.; Oyaizu, K. *Coord. Chem. Rev.* **2003**, *237*, 213–238, and references therein. (b) Dutta, S.; Basu, P.; Chakravortya, A. *Inorg. Chem.* **1993**, *32*, 5343–5348. (c) Yamamoto, K.; Oyaizu, K.; Tsuchida, E. *J. Am. Chem. Soc.* **1996**, *118*, 126656–12672. (d) Dutta, S. K.; Samanta, S.; Kumar, S. B.; Han, O. H.; Burckel, P.; Pinkerton, A. A. *Inorg. Chem.* **1999**, *38*, 1982–1988. (e) Dutta, S. K.; Kumar, S. B.; Bhattacharyya, S.; Tiekink, E. R. T.; Chaudhury, M. *Inorg. Chem.* **1997**, *36*, 4954–4960. (f) Holwerda, R. A.; Whittlesey, B. R.; Nilges, M. J. *Inorg. Chem.* **1998**, *37*, 64–68.

(27) Hoppe, E.; Limber, C.; Ziemer, B.; Mugge, C. *J. Mol. Cat. A* **2006**, *251*, 34–40.

(28) Radius, U. *Inorg. Chem.* **2001**, *40*, 6637–6642.

led to the first grafted calixarene complexes that are 1,3-disubstituted at the lower rim. Upon exposure to air, vanadium(III) centers on the grafted material oxidize, resulting in material **2c**, consisting of isolated V(V) centers confined within a pseudo-octahedral oxo environment, coordinated from the top by a calixarene moiety and from the bottom by silica surface. This grafting strategy leads to hydrolytic and oxidative stability, as well as stable site-isolation relative to a material in which vanadocalixarene sites have been physisorbed on the surface of silica using the noncovalent immobilization of precursor *p*-Bu^t−calix[4]−(OMe)(O)$_3$V═O (**1n**). The results of this paper therefore emphasize the importance of covalent connectivity to the support for formation of well-defined organometallic active sites on surfaces, even in cases when a sterically bulky ligand is used to prevent aggregation. Strong MeO→metal interactions between calixarene lower-rim substituted oxygens and metal center in **2c** are indicated by an upfield-shifted ipso carbon resonance in the ^{13}C CP/MAS spectrum. The increased of these interactions is predicted for 1,3-disubsituted complexes relative to monosubsituted complexes on the basis of simple geometric arguments that are supported by single-crystal X-ray diffraction data. This suggests a weak Lewis acidity for **2c** and bodes well for the possibility of programming chemical and stereochemical information from calixarene lower-rim substituents onto the grafted metal center in the class of grafted calixarene materials consisting of 1,3-disubstituted ligands at the lower rim.

Experimental Section

Thermogravimetric analysis (TGA) was performed on a TA Instruments TGA 2950 system using a flow of dry synthetic air at a ramp rate of 5 °C/min. Vanadium contents were determined by a previously published procedure:[4a,b] QTI elemental analysis for C and V was also performed. UV−vis spectroscopy was performed on a Varian Cary 400 Bio UV−vis spectrophotometer equipped with a Harrick Praying Mantis accessory for diffuse reflectance measurements on solids at room temperature. Compressed PTFE powders were used as a reference. Solid-state MAS and CPMAS NMR spectra were measured using a Bruker Avance 500 MHz spectrometer with a wide bore 11.7 T magnet and employing a Bruker 4 mm CPMAS probe. The spectral frequencies were 500.2, 125.7, 131.1 MHz for the ^{1}H, ^{13}C, and ^{51}V nuclei, respectively. NMR shifts are reported in parts per million (ppm) and are externally referenced to tetramethylsilane (TMS) for ^{1}H and ^{13}C and $VOCl_3$ solution in benzene for ^{51}V. Samples were typically spun at 14 kHz for both MAS and CPMAS experiments. EPR spectra were obtained using a X-band Bruker (Model EMX) EPR spectrometer. Xray structures were obtained from the Cambridge Structural Database.[29] Other model structures were built using Maestro 7.5,[30] a general purpose graphical program from Schrodinger Inc. All structures were subsequently optimized using Jaguar 6.5[31] at B3LYP/LACVP*. Orbital analysis was done using NBO 5.0.[32]

Precursor Synthesis for 1c. Precursor **1c** was prepared according to a published procedure.[13a]

Precursor Synthesis for 1n. ^{n}BuLi (1.4 mL, 2.2 mmol) was added dropwise to a THF solution (10 mL) of Bu^t−calix[4]−(OMe)$_2$(OH)$_2$ (0.75 g, 1.1 mmol) at −30 °C. $VOCl_3$ (0.1 mL, 1 mmol) was syringed into the above orange solution, and the resulting purple solution was then brought to room temperature. After the mixture was stirred overnight, the suspension was evaporated to dryness and the purple solid residue was extracted with anhydrous hexane. The hexane extract was evaporated to dryness to isolate **1n** with 70% purity. Highly purified samples of **1n** were obtained by treating saturated hexane solutions of the above crude product with trace amounts of silica gel to remove unidentified impurities and extracting the pure **1n** component into anhydrous toluene. Characterization methods: ^{1}H,^{13}C, ^{51}V NMR (see Supporting Information).

Material Synthesis for 2c. Chromatography silica gel (1.5 g, 60 Å pores, 250−500 m, Selecto) was partially dehydroxylated under dynamic vacuum at 400 °C for 24 h. The silica was directly transferred under argon to a flask containing a 0.20 mmol sample of **1c** in toluene solution. The mixture was stirred for 3 h at room temperature. The resulting solid was filtered, thoroughly washed with anhydrous toluene, followed by hexane, and dried under dynamic vacuum at 25 °C for overnight.

Material Synthesis for 2n. Chromatography silica gel (900 mg, 60 Å pores, 250−500 m, Selecto) was partially dehydroxylated under dynamic vacuum at 400 °C for 24 h. The silica was directly transferred under argon to a flask containing a 0.11 mmol sample of **1n** (as a hexane solution). The purple color of **1n** was immediately transferred from the solution to the solid. After 45 min of stirring, the solid was filtered, washed with anhydrous hexane, and dried under dynamic vacuum at 25 °C for overnight.

Acknowledgment. The authors acknowledge the U.S. DOE Office of Basic Energy Sciences (Grant DE-FG02-05ER15696). NSF CHE-0233882 funded the computing equipment used in the computational aspects of this project.

Supporting Information Available: . ^{1}H,^{13}C, ^{51}V NMR spectra for precursor **1n** and Table S1, consisting of a compilation of relevant bond distances, from single-crystal X-ray diffraction structural data on V− and Ti−calixarene complexes. This material is available free of charge via the Internet at http://pubs.acs.org.

CM803392M

(29) Allen, F. H. *Acta Crystallogr, B* **2002**, *58*, 380–388.
(30) *Maestro 7.5*; Schrodinger L.L.C.: New York, 2008.
(31) *Jaguar 6.5*; Schrodinger L.L.C.: New York, NY, 2008.
(32) (a) Glendening, E. D.; Badenhoop, J. K.; Reed, A. E.; Carpenter, J. E.; Bohmann, J. A.; Morales, C. M.; Weinhold, F. *NBO 5.0*; Theoretical Chemistry Institute, University of Wisconsin: Madison, WI, 2001. (b) Weinhold, F.; Landis, C. R. *Chem. Ed.: Res. Pract.* **2001**, *2*, 91–104 (special "Structural Concepts" issue).